Force sensing and transmission in human induced pluripotent stem-cell-derived pericytes

Iendaltseva, O.

Chapter 4

Insights into the regulation of α-smooth muscle actin expression in pericytes [1]

abstract

Depending on the location along the microvascular tree pericytes (PCs) have been divided into three subgroups: pre-capillary, mid-capillary and post-capillary PCs. Mid-capillary PCs completely lack α-SMA, while pre- and post-capillary PCs show a gradient in the α-SMA expression levels from low, next to mid-capillaries, to high closer to arterioles and venules where smooth muscle cells (SMCs) come in place. How this gradient is conditioned in the resting vasculature remains unclear.

In this chapter we assessed aspects of the α-SMA expression control in PCs by means of mechanical signals. We investigated whether such parameters like vessel diameter, basement membrane (BM) composition and stiffness can have an effect on the α-SMA recruitment to stress fibers in mural cells, as well as in SMCs. Automatic image data analysis approach was utilized to obtain uncompromised data on the α-SMA fiber formation with a single cell resolution.

Our results showed that α-SMA expression in PCs can be mainly affected by the presence of fibronectin (FN) deposits in the BM of microvessels and less by the stiffness or vessel diameter. In the mean time, SMCs are more dependent on the rigidity and allowed area for spreading

1. This chapter is based on: O. Iendaltseva, V.V. Orlova, C.L. Mummery, E. H. J. Danen and T. Schmidt, Insights into the Regulation of α-Smooth Muscle Actin Expression in Pericytes, *In preparation*

then on the FN arrangement. Notably, PCs could adapt their α-SMA cytoskeletal recruitment in response to the ECM properties. These findings may further help to unveil processes behind maintaining α-SMA expression gradient in PCs and can be used to keep PCs from obtaining contractile phenotype in cell culture.

4.1 Introduction

The important process of the exchange of gases, solvents and solutes between tissues and blood happens in the capillary beds of the circulatory system. These beds consist of the smallest vessels – arterioles, capillaries, and venules, which penetrate all organs and tissues of the human body. From them, capillaries can be further divided into three types: pre-capillaries, mid-capillaries, and post-capillaries [1] (Fig. 4.1). In some tissues arterioles give rise to metarterioles that are either directly connected to venules, or precede capillaries. The mean diameter of microvessels in this region changes from the $\sim$ 30 μm arterioles and $\sim$ 15 μm metarterioles down to $\sim$ 8 μm in diameter mid-capillaries and back up to the $\sim$ 20 μm venules [2]. Vessel tubes are formed by endothelial cells (ECs), while pericytes (PCs) and smooth muscle cells (SMCs) – the mural cells of blood microvessels, localize to the abluminal surface of these tubes. Depending on the location and morphology, PCs have been divided into three subgroups: pre-capillary, mid-capillary, and post-capillary PCs [3]. Mid-capillary PCs have the most prominent difference from the SMCs. They completely lack α-smooth muscle actin (SMA) expression, while SMCs are α-SMA positive. They have long cytoplasmic processes along the vessel with thin, perpendicular to the primary branches, secondary processes, which partially encircle the vessel in contrast to the band-like circumferential phenotype of SMCs (Fig. 4.1). Because of this clear polarity, PCs located on mid-capillaries have been defined as "true" or "approved" PCs [1, 4], while, pre- and post-capillary mural cells – as transitional PCs [3].

Transitional PCs are morphologically heterogeneous and, depending on their location, display a smooth shift from the mid-capillary PC phenotype to SMC. Besides variations in morphology, transitional PCs show a gradient in the α-SMA expression levels from low (close to the mid-capillaries) to high (next to the arterioles or venules) [4, 5] (Fig. 4.1). Due to this gradient, transitional PCs are sometimes mistakenly determined as pre- and post- capillary SMCs [6]. Indeed, distinguishing between PCs, their types and SMCs is challenging, especially in case of *in vitro* cell cultures. There is no clear "border" and no single marker that would be specific for all PCs or any subtype. Yet, the main feature that marks all types of PCs out of SMCs is their ability to support angiogenesis [7]. Recently it has been shown that human pluripotent stem cell (hPSC)-derived immature PC can be specified to either mid-capillary or pre-

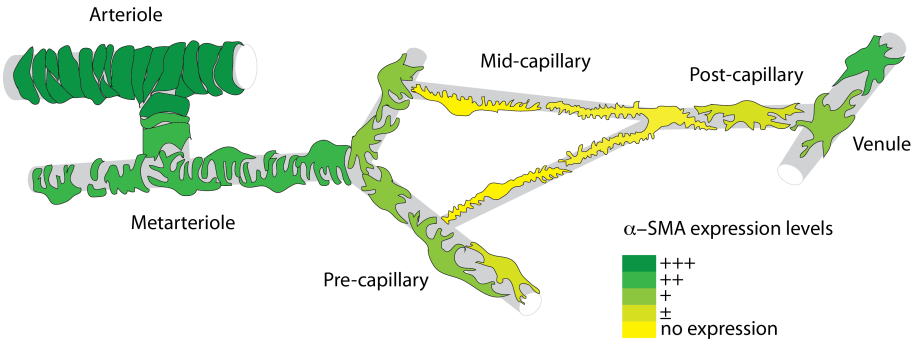

Figure 4.1: Schematic representation of the heterogeneous expression of α-SMA in pericytes of pre-, mid- and post-capillaries (adapted from [4])

capillary PC types by treatment with different combinations of growth factors (GF) [7]. Cell culture media containing platelet-derived growth factor (PDGF)-BB in combination with transforming growth factor-beta (TGF-β) induces α-SMA and Calponin 1 (CNN1)-negative PCs to up-regulate expression of smooth muscle markers like smooth muscle-specific protein 22 (SM22), α-SMA and CNN1[8, 9]. However, *in vivo* PCs expressing α-SMA and PCs lacking α-SMA can be located next to each other and sometimes even on the vessel of the same branch order [4–6]. This raises the question, how the α-SMA expression gradient is conditioned and maintained in the resting vasculature.

Here we investigated a potential influence of the mechanical aspects, such as vessel stiffness, width and spatial organization of the capillary basement membrane (BM) proteins on the regulation of the α-SMA expression and recruitment to stress fibers in PCs. We used the previously described human induced pluripotent stem cell (hiPSC)-derived PCs as a cell model resembling mid-capillary PCs, lacking α-SMA expression [8, 9]. Quantification of the α-SMA immunostaining intensity and distribution allowed us to asses not only the level of the α-SMA expression, but also the degree of its recruitment to cellular stress fibers. Our findings suggest that: i) besides chemical cues the α-SMA expression gradient in PCs is influenced by capillary mechanical properties; ii) FN deposits found in the PC-ECs interstitial layer of the capillary BM [10] may have a major contribution to the conditioning and maintaining of this gradient compared to other mechanical signals.

4.2 Methods

4.2.1 Cell culture

CD31– cells derived from the hiPSC line LUMC06iCTRL-derived (dif31), SV80 human fibroblasts, and HASM human arterial smooth muscle cells (Applied Cell Biology Research Institute, Kirkland, WA) were cultured in Dulbecco's Modified Eagle's Medium (DMEM, Gibco | Thermo Fisher Scientific, USA) supplemented with 10% fetal bovine serum (HyClone, Etten-Leur, The Netherlands), 25 U/ml penicillin and 25 µg/ml streptomycin (Invitrogen/Fisher Scientific). The CD31– cell line was used at passage 7 or 8 and cultured for 3 to 4 days before experiments. For 4 and 24 hours long cell incubation time experiments, cells were seeded at 20,000 cells per sample and for 7 day incubation – at 10,000 cells/sample. Cells were injected directly on top of the substrate area of interest to ensure persistent cell density across experiments. After incubation they were fixed 10' in 4% paraformaldehyde in PBS for further immunostaining. Gelatin and fibronectin (FN) used as cell substrates were obtained from Sigma (g2500 and f1141 respectively).

4.2.2 Immunostaining

Fixed cells were permeabilized for 10' with 0.1% Triton-X in PBS and blocked for 60' with either 1% bovine serum albumin (BSA) (Sigma, a2153), or 1% or 5% goat serum (GS) (Sigma, G6767) in PBS. α-SMA was immunostained, first, with a mouse monoclonal (clone 1A4) primary antibody against α-SMA (Sigma, A2547) in a blocking buffer o/n, followed by 3 washing steps in PBS 10' each under a gentle rocking. Secondly, the Alexa 532 conjugated secondary antibody against mouse IgG (Thermo Fisher Scientific, a11002) was applied in a blocking buffer for 2 hours. The antibody was subsequently removed with 3X 10' in PBS washing steps under rocking. Additionally, F-actin cytoskeleton of cells in a number of experiments was stained with Alexa 647 phalloidin (Thermo Fisher Scientific, a22287) of a 1:1000 concentration in PBS.

4.2.3 Microscopy

Confocal imaging was performed on a home-built setup based on an Axiovert200 microscope body (Zeiss), spinning disk unit (CSU-X1, Yokogawa) and an emCCD camera (iXon 897, Andor). IQ-software

enabled setup-control and data acquisition. Lasers of 405 nm (CrystaLaser), 488 nm (Coherent), 514 nm, 561 nm (Cobolt) and 642 nm (Spectra Physics) wavelength were coupled into the CSU via polarization maintaining single-mode fiber. Spacers on the sides of micropillar arrays allowed placing them upside down onto #0 coverslips (Menzel Glaser) with adhered cells facing down. This approach ensured reproducible cell observation within the limited working distance of a high-NA objective on an inverted microscope. For PDMS or glass 2D assays parafilm spacers were made directly on top of the glass coverslips.

4.2.4 Image analysis

The level of the α-SMA expression and the degree of it's recruitment to cellular stress fibers was assessed with the help of quantification of the α-SMA staining intensity and distribution. The quantification was done automatically with the help of a particularly designed Matlab script, comprising a call to FIJI/ImageJ (NIH, Maryland, USA) image analysis software plug-in – OrientationJ (EPFL, Switzerland)[11]. The acquired images were split into the original channels and the plug-in was used to find the orientation within the local features of the α-SMA staining distribution in the corresponding channel (Example fig. 4.2a, 4.2b). This was done by computing the so-called structure tensor for each pixel with the help of a cubic spline interpolation in the sliding over the entire image Gaussian analysis window. This window we have chosen to be 2 pixels in size for images taken with the 40x magnification objective having NA= 1.3 or 1.5 pixels for – 100x magnification and NA= 1.4 objective. The change in the window size is reasoned by the difference in the minimal diameter of the fluorophore airy pattern that can be acquired with NA= 1.3 and NA= 1.4 objectives. From the structure tensor the "coherency" value (from 0 to 1) as a ratio between the difference and the sum of the maximum and minimum tensor eigenvalues was obtained to distinguish between the isotropic and uniform regions of the image.

The picture coherency map built by the FIJI plug-in (Example fig.4.2c, 4.2d) was further processed in Matlab to find a common coherency background level outside the cell across all images that would characterize uniform regions of the image (Example 3D histograms of the coherency values distribution vs corresponding intensity per pixel for the first cell 4.2e and the second 4.2f). To mask out the cell we used an image channel of the cell F-actin. The global threshold for the channel was found

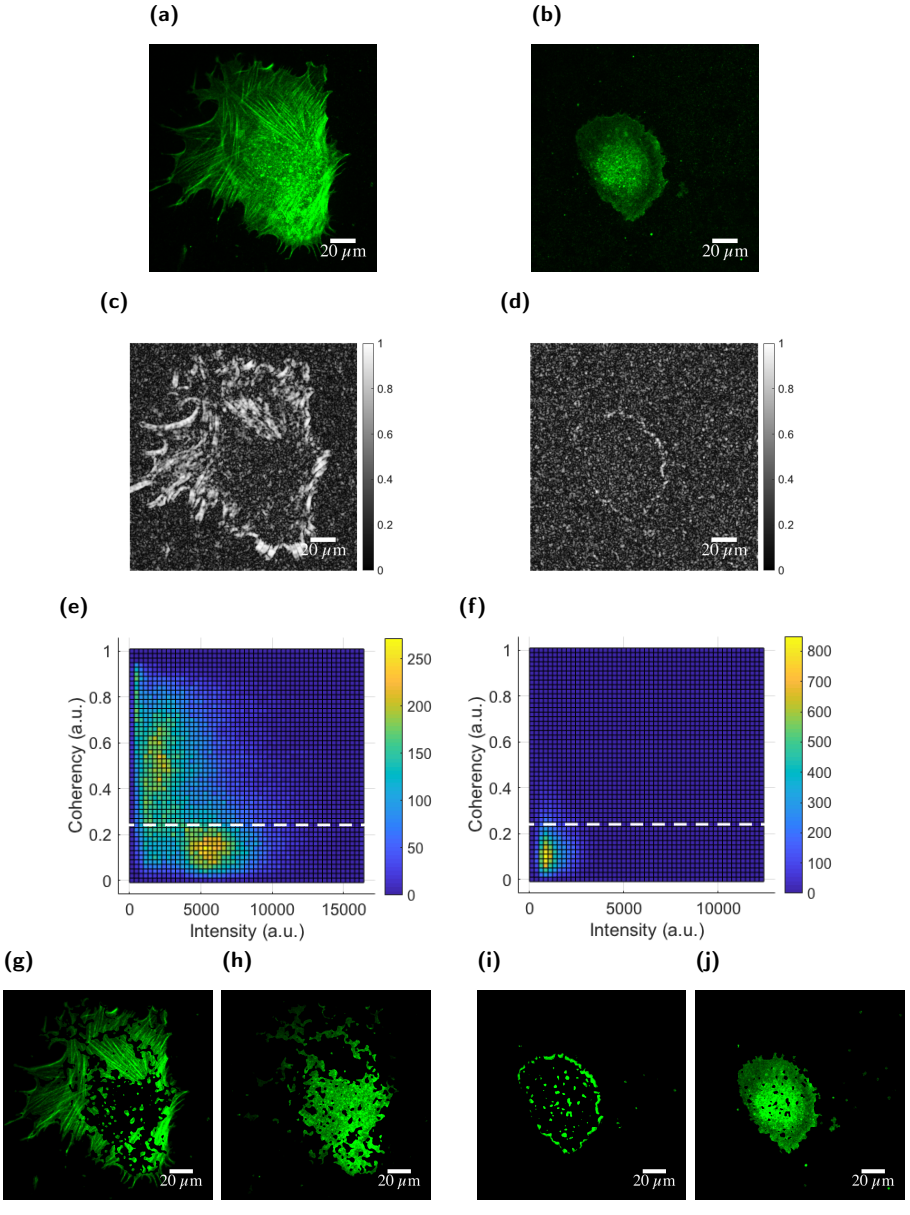

Figure 4.2: Representative images for coherency evaluation. (a, b) HASM cells with α-SMA (shown in green) recruited and not recruited to stress fibers. (c, d) Coherency maps built by the FIJI plug-in for the (a) and (b) respectively. (e, f) 3D histograms of the coherency values distribution vs corresponding intensity per pixel for the (a) and (b) respectively. (g, i) "coherent" (higher then 0,25 a.u. – dashed line on (e) and (f)) and (h, j) "non-coherent" (lower then 0,25 a.u.) areas of the α-SMA staining within the cell.

with an algorithm based on the earlier described triangle method [12]. This algorithm comprised an opportunity to manually tune the image intensity histogram offset to ensure a correct mask correlation with the cell. After the subsequent background subtraction and edges detection an image dilation and hole filling algorithms were implemented. The obtained cell mask was used to delete the cell coherency values and leave the background.

Quantified average level of maximal background values (0.25 a.u.) was further used to separate "coherent" (with fibers) (Fig. 4.2g, 4.2i) and "non-coherent" (without fibers) (Fig. 4.2h, 4.2j) regions of the α-SMA staining within the cell. Finally, the box plot graphs displaying the distribution of medians of the coherency values per cell were built. These coherency values were taken from the "coherent" regions (higher then 0.25 a.u.) of the cell. Additionally, the distributions of the percentage of these regions from the total cell area were shown. This graphs allowed us to compare the degree of α-SMA recruitment to the cell stress fibers, while the box plots showing the variation in the median values of the total α-SMA immunostaining intensity per cell could be used to estimate the level of α-SMA general expression.

4.2.5 Statistical analysis

To assess significance of the difference between two conditions, the Wilco-xon rank sum test in the Matlab program was used. This test is an equivalent to a Mann-Whitney U test.

4.3 Results

4.3.1 α-SMA expression and recruitment to stress fibers quantified by orientation analysis.

First, we investigated whether the level of α-SMA expression and the cell extracellular matrix (ECM) may influence the degree of the α-SMA recruitment to cell stress fibers during the spreading. We used SV80 human fibroblasts as an α-SMA negative control and HASM human aorta smooth muscle cells as an α-SMA positive control. As a source for PCs we used hiPSC line LUMC06iCTRL-derived PCs (CD31–) [9, 13] of an early passage that expressed very little to no α-SMA and very little SMC

markers such as (SM)22 and Calponin (CNN1), distinguishing them from SMCs.

Cells were placed on gelatin or fibronectin (FN) covered coverslips for 4 hours, fixed and stained with anti-α-SMA antibody followed by staining with an Alexa-532-coupled secondary antibody. Collected confocal images of the α-SMA fluorescent staining were used to identify the presence and the level of orientation within local features of the α-SMA staining distribution that we quantified as coherency (see Methods section). Only those areas were taken into account and considered "coherent" that had values higher then the average coherency background ($\sim$0.25 a.u.). Additionally we quantified a percentage of the "coherent" cell area from the total cell area that was analyzed (A_{coh}/A_{tot} (%)) to get a better overview of the degree of α-SMA recruitment to stress fibers.

CD31– cells on coverslips coated with gelatin had a comparable level and percentage of coherency to fibroblasts (Fig. 4.3d) (Fig. 4.3f). This level was close to the overall image background pointing on the absence of oriented features and isotropic distribution of the anti-α-SMA antibody staining inside cells (Example figures. 4.3a, b). HASM cells, in turn, had more α-SMA staining organized in fibers (Fig. 4.3c) that was also reflected in a higher level of coherency as well as the percentage of the coherent area compared to SV80 or CD31– cells (Fig. 4.3d, 4.3f). On FN coated glass coverslips overall levels of coherency both of CD31– (median value =0.33 a.u.) and SV80 (median value =0.3 a.u.) were higher then on gelatin (median value CD31– =0.31 a.u., SV80 =0.295 a.u.)(significance of the difference for SV80 cells $p<0.0005$, for CD31– $p=0.0029$)(Fig. 4.3g). Similar effect was found for the percentage of the cell coherent area (Fig. 4.3g). Notably, the level of coherency quantified for CD31– cells seeded on FN was comparable with the coherency of HASM cells seeded on gelatin (median value =0.33 a.u.) (significance of the difference $p=0.44$). However, the percentage of the coherent area within the cell quantified for SV80 and CD31– cells was similar (Fig. 4.3g).

Together, we showed that our image analysis tool for quantification of the α-SMA expression and recruitment conforms with the known data about the α-SMA expression in the tested cell lines. Interestingly, on the FN covered substrate CD31– cells showed an increased α-SMA recruitment to the F-actin cytoskeleton. This suggests a heterogeneous α-SMA expression within the PCs that can be modulated by ECM attachment.

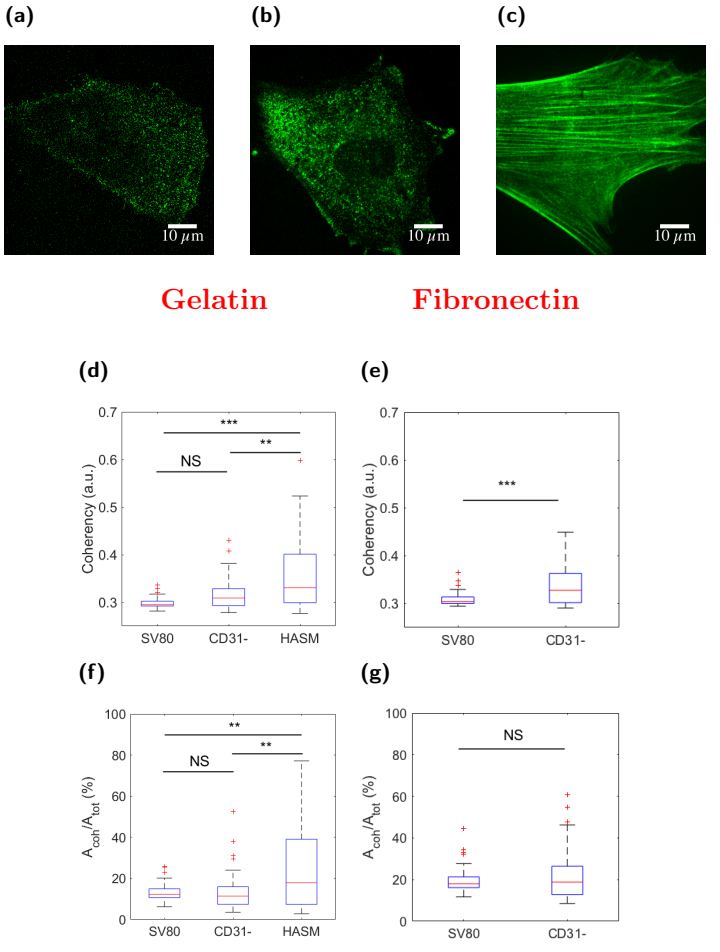

Figure 4.3: Representative images of the α-SMA immunostaining of the (a) SV80, (b) CD31– and (c) HASM cell lines seeded on gelatin coating. (d) Coherency comparison of three different human cell lines seeded on gelatin coating. (e) Coherency comparison of two different human cell lines seeded on FN coating (f, g) Respective medians of the percentage of the cell "coherent" area. Results are derived from three independent experiments performed in minimum two replicates. NS, P>0.05; *P<0.05; **P<0.005; ***P<0.0005 according to Mann - Whitney test.

4.3.2 Changes in α-SMA recruitment to stress fibers of PCs driven by growth factors.

We further investigated whether growth factors (GFs) that either induce or inhibit α-SMA expression in PCs may also influence the rate and the degree of it's recruitment to stress fibers. Additionally, we studied a potential effect from the cell ECM properties on the α-SMA recruitment in PCs treated with GFs. We used TGF-β and FGF2 in relation to two different ECM protein substrates on which the cells were placed. TGF-β is known to induce α-SMA expression [14], while FGF2 was shown to inhibit α-SMA expression in PCs [15, 16]. As substrates for CD31– cell adhesion we used FN and gelatin coatings. According to our previous findings (see Chapter 3) PC have a strong affinity towards FN, while gelatin is a recommended substrate for culturing PCs or SMCs.

The effect of GF treatment on α-SMA recruitment to stress fibers in CD31– cells was studied in two set-ups. In the first set-up CD31– cells were seeded on top of the coverslips covered with either gelatin or FN for 24 hours in either normal media, or a media containing two different amounts of TGF-β (1ng/ml and 10ng/ml), or a media with 5ng/ml concentration of FGF2 (Fig. 4.4a). After incubation cells were fixed and immunostained with the anti-α-SMA antibody, followed by imaging and coherency analysis of the image data (Fig. 4.4). In the second set-up CD31– cells were, first, incubated in a petridish with gelatin or FN coating for four days in a media containing either 1ng/ml concentration of TGF-β, or 10ng/ml – TGF-β, or 5ng/ml FGF2, as well as, in a normal media. After these four days cells from the gelatin coated petridishes were trypsinized and seeded for 4 hours in normal media on coverslips coated with gelatin, and cells from the FN coated petridishes – on coverslips coated with FN (Fig. 4.5a). Subsequently CD31– cells were fixed and the coherency of anti-α-SMA immunostaing distribution was quantified (Fig. 4.5). This approach allowed us to study: (i) the influence of the ECM on the PC response to treatment with GFs for a short term; (ii) the change in the speed of α-SMA recruitment to the stress fibers after prolonged exposure to GFs.

Local coherency quantification results obtained from the CD31– cells incubated with GFs for 24 hours didn't show a significant difference from the control sample on gelatin (Fig. 4.4b)(control=0.314 a.u., 1ng/ml TGF-β=0.316 a.u., 10ng/ml TGF-β=0.36 a.u., FGF2=0.33 a.u. with the significance of the difference $p>0.05$ for all samples) as well as on

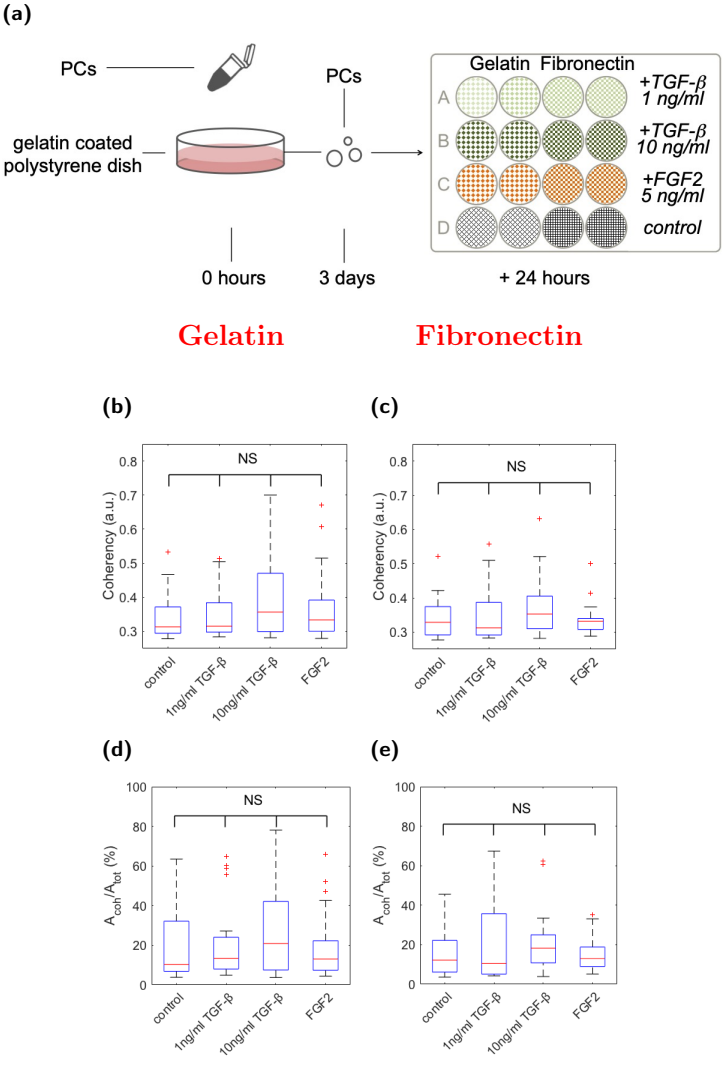

Figure 4.4: (a) Schematic representation of the experiment setup. (b, c) Coherency quantification results of CD31– cells incubated with GFs for 24 hours on gelatin (b) and FN (c). (d, e) Respective medians of the "coherent" area percentage within the total cell area of CD31– cells incubated on gelatin (d) or FN (e). Results are derived from two independent experiments performed in minimum three replicates. NS, P>0.05; *P<0.05; **P<0.005; ***P<0.0005 according to Mann - Whitney test.

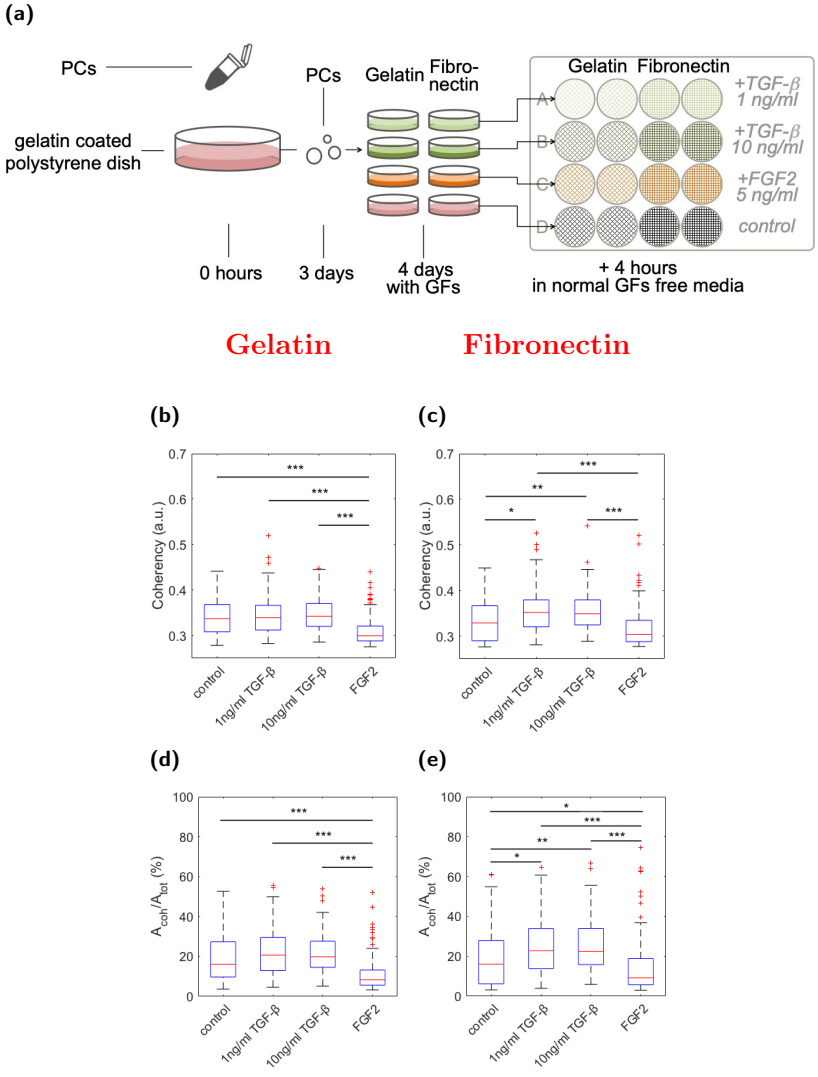

Figure 4.5: (a) Schematic representation of the experiment setup. (b, c) Coherency quantification results of CD31– cells treated with GFs for 4 days and fixed after 4 hours incubation in full media on gelatin (b) and FN (c). (d, e) Respective medians of the "coherent" area percentage within the total cell area of CD31– cells incubated on gelatin (d) or FN (e). Results are derived from two independent experiments performed in minimum three replicates. NS, P>0.05; *P<0.05; **P<0.005; ***P<0.0005 according to Mann - Whitney test.

FN substrates (Fig. 4.4c) (control=0.33 a.u., 1ng/ml TGF-β=0.312 a.u., 10ng/ml TGF-β=0.35 a.u., FGF2=0.33 a.u. with the significance of the difference p>0.05 for all samples). Also, coherency quantification results on gelatin were not significantly different from the results on FN in any GF condition. This data suggests a low or no influence from the short treatment with GFs on the recruitment of α-SMA to the F-actin cytoskeleton of CD31– cells both on gelatin or on FN.

Nevertheless, prolonged treatment with GFs affected the recruitment of α-SMA in CD31– cells (Fig. 4.5). Four days of incubation with TGF-β resulted in increased coherency levels of CD31– cells seeded on FN compared to the control sample and decreased – for CD31– cells treated with FGF2 (Fig. 4.5c) (control=0.33 a.u., 1ng/ml TGF-β=0.35 a.u., 10ng/ml TGF-β=0.35 a.u., FGF2=0.3 a.u.). This was also reflected in the quantification of the respective coherent area of CD31– cells seeded on FN (Fig. 4.5e). However, on gelatin only the treatment with FGF2 resulted in coherency levels different from the control sample (Fig. 4.5b) (control=0.337 a.u., 1ng/ml TGF-β=0.34 a.u., 10ng/ml TGF-β=0.34 a.u., FGF2=0.29 a.u. with the significance of the difference p>0.05 for TGF-β treated samples compared to the control). Treatment with TGF-β failed to increase the recruitment rate of α-SMA in CD31– cells incubated on gelatin (Fig. 4.5b). The same situation was observed from the percentage quantification of the coherent area from the total cell area of CD31– cells seeded on gelatin (Fig. 4.5c). Nevertheless, coherency quantification results obtained on gelatin were not significantly different from the results on FN in any GF condition. The coherency quantification results obtained for the samples treated for 24 hours or 4 days with 1 ng/ml TGF-β were not different form those treated with 10 ng/ml TGF-β both on FN or gelatin (Fig. 4.4, 4.5).

Taken together, we showed that prolonged treatment with GFs affects not only the expression of α-SMA in CD31– cells, but also the rate of it's recruitment to stress fibers of cells. Notably, CD31– cells treated with FGF2 for four days either on FN or gelatin both showed a decrease in the coherency values (Fig. 4.5c, b) to the level obtained earlier for human fibroblasts (Fig. 4.3), confirming an inhibitory action of the FGF2 on the α-SMA.

4.3.3 Inhibition of the time dependent increase in the α-SMA expression and recruitment to stress fibers in PCs on patterned FN substrates.

Here we investigated further the effect from the ECM properties on PCs expression and recruitment of the α-SMA. PCs bind and can apply forces on capillaries through BM proteins (Chapter 3). The interstitial layer of the BM in between PCs and ECs comprises LM and FN. FN is organized in small patches embedded into the LM layer and these patches may play a role of adhesion points for PCs (see Chapter 3) [10, 17, 18] (Fig. 1.1). We have seen that PCs are able to sense the variation in the stiffness of FN patches and respond by changing, sometimes dramatically, their traction forces, spreading area and the size of cell matrix adhesions. Thus, we studied whether the gradient of the α-SMA expression in PCs observed on the different parts of the microvasculature can be mediated by the diameter of the microvessel, the stiffness of it's BM and the presence of FN patches in the interstitial layer of the BM.

First, we examined whether FN organized in patches in the BM can influence the α-SMA expression and recruitment to stress fibers in CD31– cells. We compared CD31– cells seeded on the monolayer of FN vs CD31– cells seeded on our model of the PC-EC interstitial layer of the BM where FN was exposed to cells in a form of 2 μm diameter spots surrounded by LM (see Chapter 2, Fig. 2.2c). We tracked changes in the morphology of the early passage (passage 7) CD31– cells plated on a gelatin coated polystyrene dish over four days after thawing. As can be seen from the representative images obtained after 24 hours and 4 days of incubation (Fig. 4.6a), CD31– cells became larger and changed their rhomboid shape to a more typical for SMCs morphology with longer aligned cell bodies. These CD31– cells were further splitted and seeded either on a PDMS flat surface prepared in the ratio 1:10 crosslinker:base and stamped with FN monolayer or with an earlier described pattern of FN dots surrounded by LM (Fig. 2.2c). Subsequently, one sample of CD31– cells seeded on the FN monolayer was fixed after 24 hours and the second one – after 7 days. Cd31– cells seeded on the patterned PDMS substrate were fixed after 7 days of incubation (Fig. 4.6a – the scheme of the experiment). All samples were further simultaneously permeabilized and immunostained with anti-α-SMA antibody.

Local coherency quantification results (Fig. 4.6b) revealed CD31– cells that undertook the SMCs like morphology have got a higher level

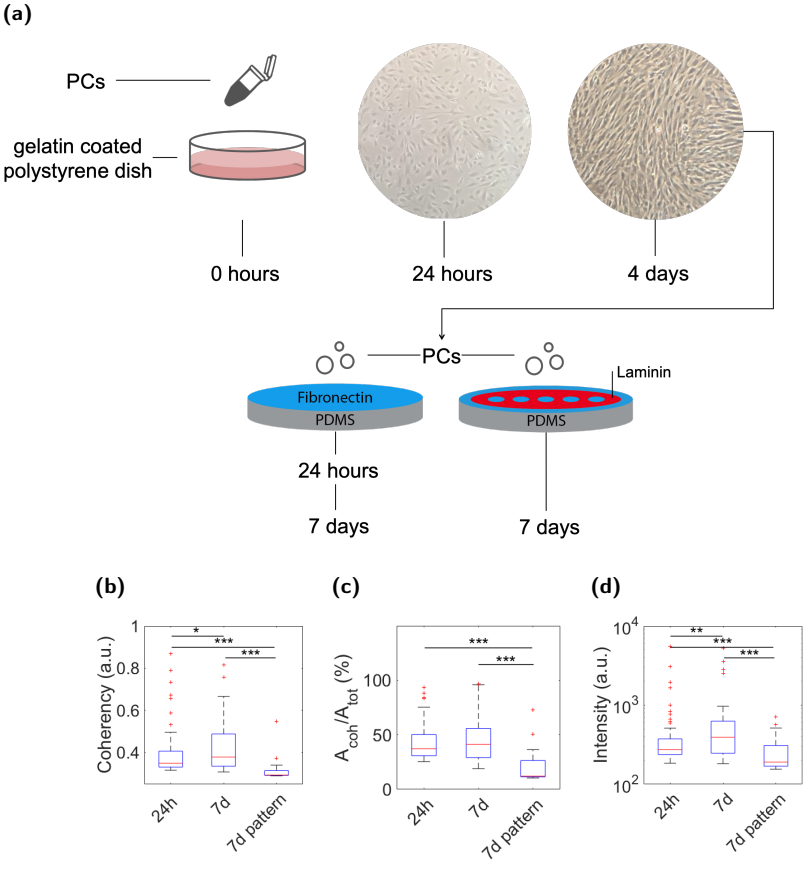

Figure 4.6: (a) Schematic representation of the experiment setup and the CD31– cell morphology after 24 hours of incubation on gelatin coated polystyrene dishes and 4 days. (b) Coherency quantification results for CD31– used after 4 days of incubation in a polystyrene dish and placed on either FN glass coverslips covered with FN monolayer for 24 hours and 7 days or on a PDMS flat surface for 7 days prepared in the ratio 1:10 crosslinker:base and stamped with an earlier described pattern of FN dots surrounded by LM (Fig. 2.2c). (c) Respective medians of the percentage of the cell "coherent" area. (d) Supportive median values of the α-SMA immunostaining intensities obtained from the total cell area that was analyzed per image for each condition. Results are derived from one experiment performed in two replicates. NS, P>0.05; *P<0.05; **P<0.005; ***P<0.0005 according to Mann - Whitney test.

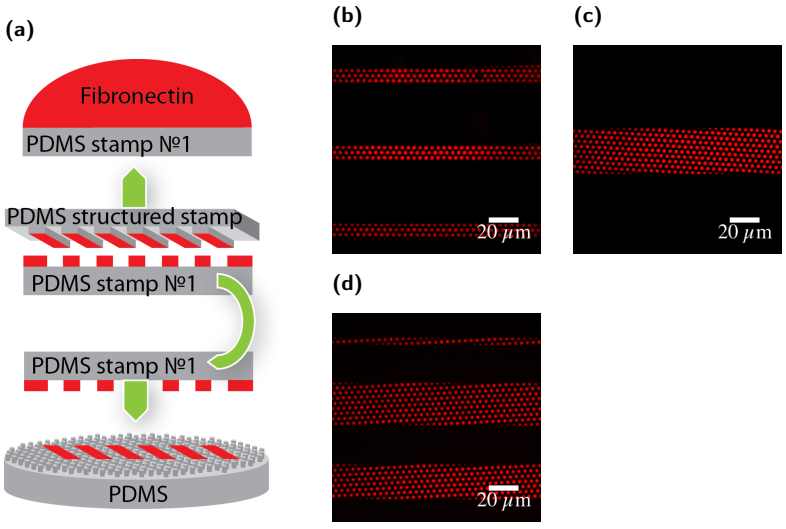

Figure 4.7: FN line pattern generation on top of the PDMS micropillar arrays. (a) A FN line microcontact printing scheme. (b – d) representative images of the different width FN (red) line stamping results on top of the micropillar arrays

of coherency (median value =0.35 a.u.) after 24 hours of incubation on FN, compared to the aforementioned result obtained from CD31– cells that were used before the change in their morphology (median value =0.33 a.u.) (significance of the difference p=0.003) (Fig. 4.4c). The coherency level appeared even higher in CD31– cells fixed after 7 days of incubation on a FN monolayer (Fig. 4.6b). Notably, CD31– cells plated on the PDMS surface patterned with FN dots embedded into LM after 7 days of incubation showed much lower level of coherency (median value =0.294) then the same cells plated on a FN monolayer (Fig. 4.6b). This value was comparable to the earlier obtained result for the α-SMA negative fibroblast cell line – SV80 (Fig. 4.3d, e). A similar effect was observed in the percentage evaluation of the coherent area within the cells (Fig. 4.6c). CD31– cells seeded on a pattern of FN dots surrounded by LM showed a lower percentage of the coherent area then CD31– cells on FN monolayer after 7 days of incubation, telling that lower amount of α-SMA fibers was formed. This data suggests an inhibitory effect from the FN organized in patches in the capillary BM on the α-SMA recruitment to the F-actin cytoskeleton of PCs.

Further, we studied a possible influence of the capillary stiffness or diameter on the α-SMA expression levels in PCs on different parts of the microvascular tree. PDMS micropillar arrays of three different stiffness (11.6 kPa, 47.2 kPa and 137 kPa) were developed and stamped with tree different patterns of FN: homogeneous layer, 30 μm wide FN lines and 10 μm wide FN lines (Fig. 4.7). This allowed us to introduce such parameters like varying substrate stiffness and restricted area for the cell adhesion into our system, representing the capillary rigidity and diameter variation. The pillars had the same diameter and arrangement as FN spots surrounded by LM on the PDMS flat surface in the previous experiment. CD31– cells were seeded onto PDMS micropillar arrays and fixed after either 4 hours of incubation or 7 days. As a control cell line for the immunostaining results we used HASM cells that were allowed to spread on PDMS micropillar arrays for 7 days. All samples were permeabilized and immunostained with anti-α-SMA antibody simultaneously. The coherency analysis revealed a low level of orientation within the CD31– cells local anti-α-SMA staining distribution on all stiffness. This effect was observed in all samples fixed after 4 hours as well as after 7 days of incubation (Fig. 4.8, 4.9, 4.10). A slight drop in the coherency level of CD31– cells was observed after 7 days of incubation on 137 kPa micropillar arrays with homogeneous stamping (from median value 0.31 to 0.306 with the significance of the difference p=0.0042) (Fig. 4.8a vs 4.8b), on 11.6 kPa arrays with 30 μm wide line stamping (from median value 0.306 to 0.303 with the significance of the difference p=0.012) (Fig. 4.9a vs 4.9b) and on 11.6 kPa and 47.2 kPa stiff arrays with 10 μm wide FN line stamping (from median value 0.31 to 0.308 with the significance of the difference p=0.010 and from – 0.304 to 0.29 with the significance of the difference p=0.022 respectively) (Fig. 4.10a vs 4.10b), compared to the results obtained after 4 hours of incubation. Notably, coherency levels were always the highest for CD31– cells incubated for 4 hours on 137 kPa micropillar arrays (Fig. 4.8a, 4.9a, 4.10a), but the difference became less prominent after 7 days of incubation (Fig. 4.8b, 4.9b, 4.10b). Nevertheless, HASM cells in total showed higher levels of coherency, obtained after 7 days of incubation, than CD31– cells after 4 hours or 7 days. The same was observed from the quantification of the coherent area persentage within cells. On avarage after 7 days of incubation CD31– cells had a lower amount of α-SMA fibers than HASM cells (Fig. 4.8e vs 4.8f, 4.9e vs 4.9f, 4.10e vs 4.10f). Interestingly, on 47.2 kPa

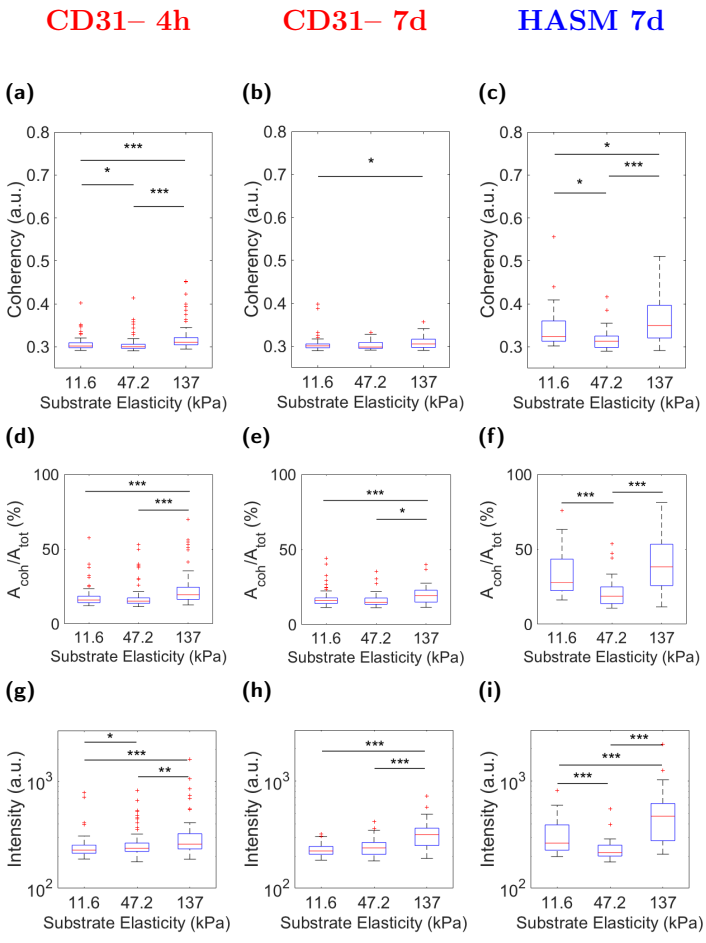

Figure 4.8: (a – b) Coherency quantification results of CD31– seeded for 4 hours (a) and for 7 days (b) on PDMS micropillar arrays of three different rigidities with homogeneous FN stamping, compared to the results of the α-SMA positive control cell line – HASM (c) after 7 days of incubation. (d – f) Respective medians of the "coherent" area percentage within the total cell area of CD31– (d, e) and HASM cells (f). (g – h) Supportive median values of the α-SMA immunostaining intensities obtained from the total cell area that was analyzed per image for each condition. Results are derived from one experiment performed in two replicates. NS, P>0.05; *P<0.05; **P<0.005; ***P<0.0005 according to Mann - Whitney test.

stiff pillars the local orientation values of the anti-α-SMA staining distribution in HASM cells were lower than on 11.6 kPa or 137 kPa arrays, indicating an overall lower α-SMA recruitment degree to the stress fibers

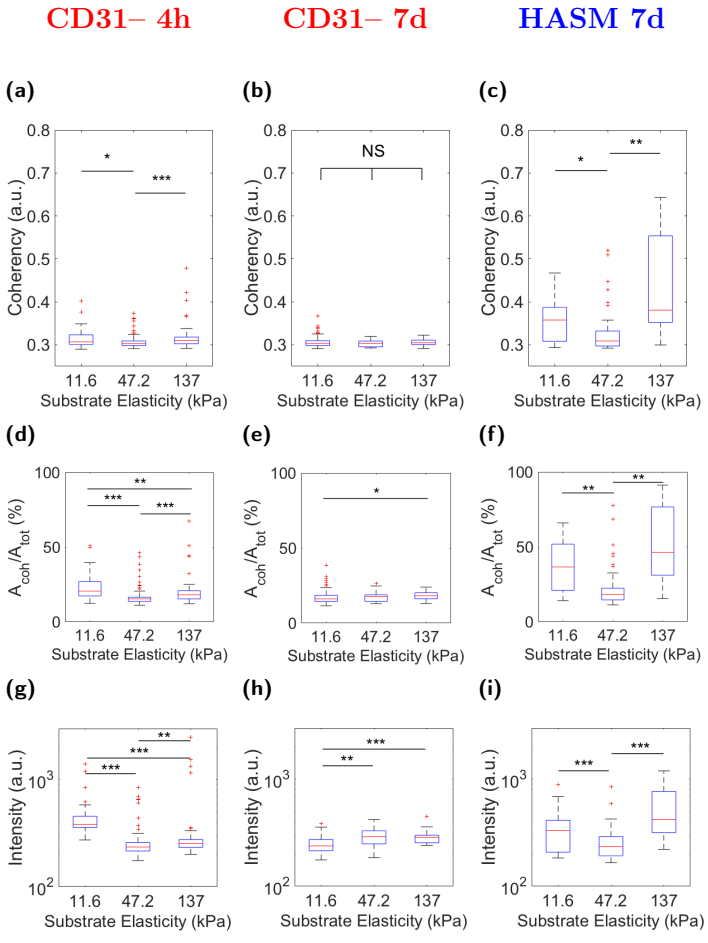

Figure 4.9: (a – b) Coherency quantification results of CD31– seeded for 4 hours (a) and for 7 days (b) on PDMS micropillar arrays of three different rigidities with 30 μm line FN stamping, compared to the results of the α-SMA positive control cell line – HASM (c) after 7 days of incubation. (d – f) Respective medians of the "coherent" area percentage within the total cell area of CD31– (d, e) and HASM cells (f). (g – h) Supportive median values of the α-SMA immunostaining intensities obtained from the total cell areas that were analyzed per image for each condition. Results are derived from one experiment performed in two replicates. NS, P>0.05; *P<0.05; **P<0.005; ***P<0.0005 according to Mann - Whitney test.

on this intermediate stiffness (47.5 kPa) than on soft (11.6 kPa) or stiff (137 kPa) substrates (Fig. 4.8c, 4.9c, 4.10c).

This data shows that the presence of FN deposits in the BM of ca-

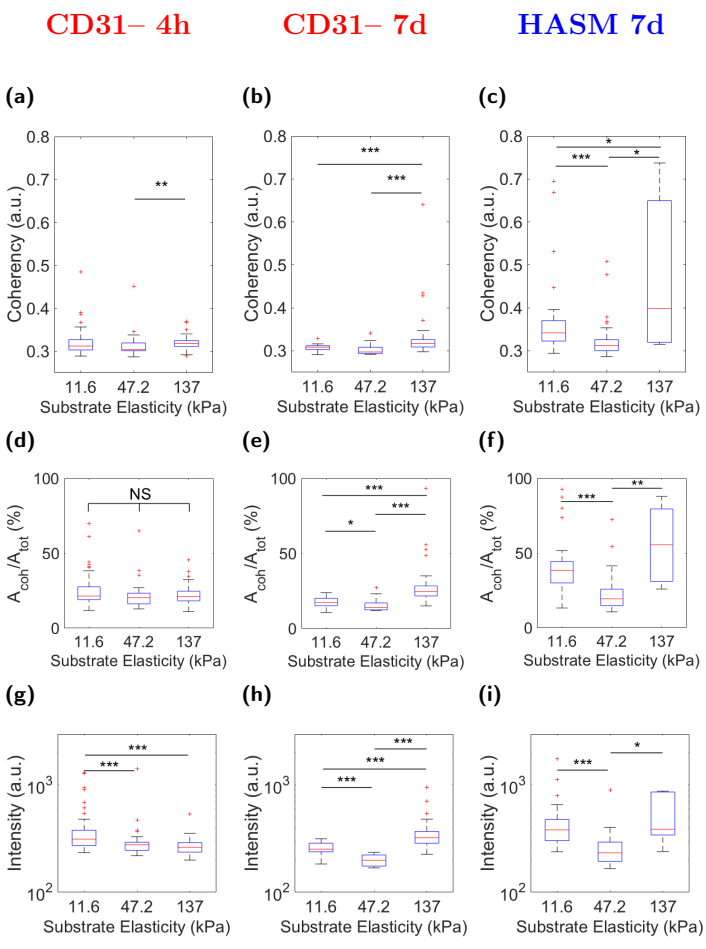

Figure 4.10: (a – b) Coherency quantification results of CD31– seeded for 4 hours (a) and for 7 days (b) on PDMS micropillar arrays of three different rigidities with 10 μm line FN stamping, compared to the results of the α-SMA positive control cell line – HASM (c) after 7 days of incubation. (d – f) Respective medians of the "coherent" area percentage within the total cell area of CD31– (d, e) and HASM cells (f). (g – h) Supportive median values of the α-SMA immunostaining intensities obtained from the total cell areas that were analyzed per image for each condition. Results are derived from one experiment performed in two replicates. NS, P>0.05; *P<0.05; **P<0.005; ***P<0.0005 according to Mann - Whitney test.

pillaries has an α-SMA inhibitory effect on PCs and less on SMCs cells. Taken together our results suggest an adaptable expression/cytoskeletal recruitment of α-SMA in PCs, which can be modulated by the ECM

properties. In the presence of FN deposits restricted to the 2 μm spot size, CD31– cells maintain a low level of localized α-SMA expression in stress fibers of and the influence from the capillary stiffness or diameter appears to be minor. By contrast, HASM cells induced α-SMA localization in stress fibers on stiff substrates irrespective of patterning.

4.4 Discussion

PCs show different levels of α-SMA expression depending on their location along the vascular tree [4–6]. *In vivo* and *in vitro* studies on PCs and other cell types show that α-SMA expression is largely affected by soluble factors, but also can be attenuated by mechanical stimuli like substrate stiffness and ECM. Taking into the account that the change of the capillary order is accompanied by the change in it's diameter, inside blood pressure, BM thickness and protein composition, PCs experience different mechanical signals on different parts of the microvascular tree and this may have an influence on the α-SMA expression. Earlier findings already pointed on a special role of ECM mechanical properties in the α-SMA regulation in myofibroblasts [19] as well as in mesenchymal stem cells [20]. Whether and how do these factors combine to condition α-SMA expression gradient in PCs in the resting vasculature remains unclear.

The main soluble factor inducing α-SMA expression in PCs is TGF-β. It has been shown to be essential for mural cell maturation into vascular SMCs [17]. PCs and ECs both express TGF-β and have TGF-β receptors on them. However, its activation from a latent proform happens when the two cell types come into contact with each other [1, 21]. How the effect from TGF-β activation is further balanced out in PCs to result in gradual increase of the α-SMA on different parts of the vascular tree is not well defined. Here we tested whether deviating levels of the α-SMA in PCs could be a consequence of TGF-β gradient in vasculature. Obtained data showed that treatment with various concentrations of TGF-β did not result in a deviating expression or recruitment rate of the α-SMA to stress fibers in PCs. Same result was obtained when two different treatment times were compared suggesting that growth factor control may not be sufficient for fine-tuning the α-SMA expression levels. Nevertheless, we noticed that the effect from the TGF-β treatment was dependent on the ECM protein coating of the substrate on which PCs

were placed. Treatment was more effective on FN, resulting in a higher levels of α-SMA recruitment rate to stress fibers. Similar observation was made by Chen and Hinz for mesenchymal stem cells [22]. They admitted that FN substrate coating in general favored α-SMA fibrogenesis in comparison to gelatin or pronectin. Kim and Gumbiner in turn reported that cell adhesion to FN promotes YAP nuclear accumulation through negative regulation of Hippo signaling pathway [23]. This can partially explain our results, taking into the account a direct relation between YAP/TAZ nuclear translocation and α-SMA expression reported earlier for mesenchymal stem cells and fibroblasts [20, 24].

FN is present in small amounts in the capillary BM, distributed in micron-sized deposits around the LM rich PC-EC interstitia. When PCs and ECs come into contact, PCs noticeably downregulate their FN expression levels, while ECs upregulate [25]. In 3D cell culture it has been shown that activated TGF-β from the PC-EC contact induces ECM production by ECs, yet, not the FN expression [26]. Limiting the amount of FN in the BM can be a key to the control over the α-SMA expression in PCs. Here we showed that α-SMA was upregulated over time in PCs originally α-SMA negative, placed on a stiff substrate of the culture dish with a FN monolayer. However, α-SMA levels were maintained or even downregulated by placing PCs on a pattern of 2 μm FN dots embedded into the LM monolayer. In the previous chapter we also showed a strong preference of PCs towards FN over LM. PCs mainly formed their cell-matrix contacts on FN dots and not on LM, when cultured on a patterned substrate. This behavior resulted in a limited size of their focal adhesions in comparison to a protein monolayer. Similar dependence between limited focal adhesion size and a low α-SMA recruitment to stress fibers was reported earlier for myofibroblasts. Authors could inhibit α-SMA recruitment by restricting cell focal adhesions to a size of printed ECM dots [19]. Taken together, there is an evidence that α-SMA recruitment to stress fibers in PCs can be affected by the amount of available FN and by its spatial arrangement.

Notably, in the presence of FN dot pattern, created by the functionalization of PDMS micropillars, CD31– failed to develop α-SMA fibers and didn't show a prominent dependence on the variation in substrate stiffness or available area for spreading. In contrast, HASMs maintained the ability to form α-SMA fibers on micropillar arrays and responded to the deviating stiffness and available area for spreading with different α-SMA

recruitment rates, yet higher then in PCs. This data demonstrates that after full maturation of PCs into SMCs they loose the ability to adjust α-SMA expression levels in response to the FN arrangement in the BM and become more dependent instead on vessel stiffness and diameter.

In this study we showed that our data analysis approach gives a benefit of gaining an uncompromised quantification information not only on the general α-SMA expression levels in cells, but also on the α-SMA recruitment degree to stress fibers, rate and total ratio with a single cell resolution. Such approach also can come into help when limited amount of cells is available, or when two conditions are being compared on the same sample, or when a dynamic live cell data needs to be assessed. Our findings may help to unveil processes behind maintaining α-SMA expression gradient in PCs and can be used to keep PCs from obtaining contractile phenotype in cell culture.

Bibliography

[1] Annika Armulik, Guillem Genové and Christer Betsholtz. « Pericytes: developmental, physiological, and pathological perspectives, problems, and promises. » In: *Dev. Cell* 21.2 (2011), pp. 193–215. ISSN: 1534-5807.

[2] Bruce M Koeppen. *Berne & Levy Physiology*. 6th ed., updated ed. Philadelphia, PA: Mosby/Elsevier, 2009. ISBN: 9780323278669.

[3] K.W. Zimmermann. « Der feinere bau der blutcapillares ». In: *Z. Anat. Entwickl.* 68 (1923), pp. 3–109.

[4] V Nehls and D Drenckhahn. « Heterogeneity of microvascular pericytes for smooth muscle type alpha-actin. » In: *JCB* 113.1 (1991), pp. 147–154. ISSN: 0021-9525.

[5] Roger Grant et al. « Organizational hierarchy and structural diversity of microvascular pericytes in adult mouse cortex ». In: *J Cereb Blood Flow Metabolism* 39.3 (2017), pp. 411–425. ISSN: 0271-678X.

[6] Robert A Hill et al. « Regional Blood Flow in the Normal and Ischemic Brain Is Controlled by Arteriolar Smooth Muscle Cell Contractility and Not by Capillary Pericytes. » In: *Neuron* 87.1 (2015), pp. 95–110. ISSN: 0896-6273.

[7] Akhilesh Kumar et al. « Specification and Diversification of Pericytes and Smooth Muscle Cells from Mesenchymoangioblasts ». In: *Cell Reports* 19.9 (2017), pp. 1902–1916. ISSN: 2211-1247.

[8] Valeria V Orlova et al. « Functionality of Endothelial Cells and Pericytes From Human Pluripotent Stem Cells Demonstrated in Cultured Vascular Plexus and Zebrafish Xenografts ». In: *Arteriosclerosis Thrombosis Vasc Biology* 34.1 (2014), pp. 177–186. ISSN: 1079-5642.

[9] Valeria V Orlova et al. « Generation, expansion and functional analysis of endothelial cells and pericytes derived from human pluripotent stem cells. » In: *Nat Protoc* 9.6 (2014), pp. 1514–31. ISSN: 1750-2799.

[10] PJ Courtoy and J Boyles. « Fibronectin in the microvasculature: localization in the pericyte-endothelial interstitium. » In: *J. Ultrastruct. Res.* 83.3 (1983), pp. 258–73. ISSN: 0022-5320.

[11] Z. Püspöki et al. « Transforms and Operators for Directional Bioimage Analysis: A Survey ». In: *Focus on Bio-Image Informatics*. Ed. by W.H. De Vos, S. Munck and J.-P. Timmermans. Vol. 219. Advances in Anatomy, Embryology and Cell Biology. Springer International Publishing, May 2016. Chap. 3, pp. 69–93.

[12] GW Zack, WE Rogers and SA Latt. « Automatic measurement of sister chromatid exchange frequency. » In: *J. Histochem. Cytochem.* 25.7 (1977), pp. 741–53. ISSN: 0022-1554.

[13] C. Dambrot et al. « Polycistronic lentivirus induced pluripotent stem cells from skin biopsies after long term storage, blood outgrowth endothelial cells and cells from milk teeth ». In: *Differentiation* 85.3 (2013), pp. 101–109. ISSN: 0301-4681.

[14] MM Verbeek et al. « Induction of alpha-smooth muscle actin expression in cultured human brain pericytes by transforming growth factor-beta 1. » In: *Am. J. Pathol.* 144.2 (1994), pp. 372–82. ISSN: 0002-9440.

[15] Michael Papetti et al. « FGF-2 antagonizes the TGF-beta1-mediated induction of pericyte alpha-smooth muscle actin expression: a role for myf-5 and Smad-mediated signaling pathways. » In: *Invest. Ophthalmol. Vis. Sci.* 44.11 (2003), pp. 4994–5005. ISSN: 0146-0404.

[16] Gregory J Sieczkiewicz and Ira M Herman. « TGF-β signaling controls retinal pericyte contractile protein expression ». In: *Microvascular research* 66.3 (2003), pp. 190–196. ISSN: 0026-2862.

[17] Annika Armulik, Alexandra Abramsson and Christer Betsholtz. « Endothelial-pericyte interactions. » In: *Circ. Res.* 97.6 (2005), pp. 512–23. ISSN: 0009-7330.

[18] Ethan A Winkler, Robert D Bell and Berislav V Zlokovic. « Central nervous system pericytes in health and disease ». In: *Nature Neuroscience* 14.11 (2011), pp. 1398–1405. ISSN: 1097-6256.

[19] Jérôme M Goffin et al. « Focal adhesion size controls tension-depen-dent recruitment of α-smooth muscle actin to stress fibers ». In: *JCB* 172.2 (2006). ISSN: 0021-9525.

[20] Nilesh P Talele et al. « Expression of α-Smooth Muscle Actin Determines the Fate of Mesenchymal Stromal Cells ». In: 4.6 (2015), pp. 1016–1030. ISSN: 2213-6711.

[21] Y Sato. « Inhibition of endothelial cell movement by pericytes and smooth muscle cells: activation of a latent transforming growth factor-beta 1-like molecule by plasmin during co-culture ». In: 109.1 (1989), pp. 309–315. ISSN: 0021-9525.

[22] Chen Li et al. « MicroRNA-21 preserves the fibrotic mechanical memory of mesenchymal stem cells ». In: 16.3 (2016), pp. 379–389. ISSN: 1476-1122.

[23] Nam-Gyun Kim and Barry M Gumbiner. « Adhesion to fibronectin regulates Hippo signaling via the FAK-Src-PI3K pathway ». In: *JCB* 210.3 (2015), pp. 503–515. ISSN: 0021-9525.

[24] Fei Liu et al. « Mechanosignaling through YAP and TAZ drives fibroblast activation and fibrosis ». In: *Am J Physiol-lung C* 308.4 (2015), pp. L344–L357. ISSN: 1040-0605.

[25] Amber N Stratman et al. « Pericyte recruitment during vasculogenic tube assembly stimulates endothelial basement membrane matrix formation. » In: *Blood* 114.24 (2009), pp. 5091–101. ISSN: 0006-4971.

[26] JA Madri. « Phenotypic modulation of endothelial cells by transforming growth factor-beta depends upon the composition and organization of the extracellular matrix ». In: 106.4 (1988), pp. 1375–1384. ISSN: 0021-9525.

BIBLIOGRAPHY